Energy 73 (2014) 475–483

Contents lists available at ScienceDirect

Energy

journal homepage: www.elsevier.com/locate/energy

Exergy analysis and working fluid selection of organic Rankine cycle for low grade waste heat recovery

R. Long, Y.J. Bao, X.M. Huang*, W. Liu*

School of Energy and Power Engineering, Huazhong University of Science and Technology, Wuhan 430074, China

ARTICLE INFO

Article history:
Received 11 November 2013
Received in revised form
17 April 2014
Accepted 10 June 2014
Available online 3 July 2014

Keywords:
Organic Rankine cycle (ORC)
Exergy efficiency
Heat recovery

ABSTRACT

The internal and external exergy efficiencies are adopted to analyze the impact of working fluids on the performance of the organic Rankine cycle, and a simplified internal exergy efficiency model is proposed to indicate this impact. The calculation results show that the thermophysical properties of the working fluid have little impact on internal exergy efficiency, but they do play an important role in determining external exergy efficiency. Under the same heat source, the internal exergy efficiency of the ORC (organic Rankine cycle) will increase for all working fluids, whereas the characteristics of the external exergy efficiency exhibit parabolic-like curves with the increase of evaporation temperature. By taking exergy efficiency as an objective function, an optimal analysis based on a genetic algorithm is conducted to illuminate the impact of working fluids on internal and external exergy efficiencies. The optimization results show that the selection of working fluids depends greatly on optimal evaporation temperature. Working fluids with lower critical temperature lead to a higher optimal evaporation temperature, which results in higher overall exergy efficiency. Therefore, the present study on selecting working fluids for organic Rankine cycle systems may have potential application in low grade waste heat recovery systems.

1. Introduction

The utilization of low grade waste heat has attracted much interest following concerns regarding the shortage of fossil energy, the depletion of fossil fuels, and global warming. Energy storage coupled with low grade renewable energy and different thermodynamic cycles can efficiently relieve such issues [1–5]. As to the thermodynamic cycles, researchers have proposed several solutions to convert low grade heat resources into electricity, such as the ORC (organic Rankine cycle), Kalina cycle, supper critical CO_2 cycle, triangle cycle, and heat pipe technology [6–9]. Among them, ORC is the relatively more practical method for waste heat recovery, and it has been adopted in many industrial applications [10]. Numerous studies have been dedicated to using ORC to utilize and recover heat from various heat resources, for instance, solar energy, exhaust gas from internal combustion engines, and geothermal resources [11–15].

The main difference from the traditional Rankine cycle is that an organic substance is used as the working fluid in ORC. Both the chemical and physical properties of organics have significant impacts on system's efficiency and net power output, which much research is focused on. Thermal efficiency of the ORC is often adopted as the criterion for screening the working fluids. Hung et al. [16] shed light on that different slopes and shapes of saturation vapor curves were the most crucial characteristics of working fluids for ORCs, and that isentropic fluids were the most suitable for recovering low temperature waste heat. In later research, Hung et al. [17] found dry fluids could lead to a superheated state of vapor at the exit of the expander, reducing the network area in the T–s diagram, as well as increasing the cooling load of the condenser. Liu et al. [18] elucidated that thermal efficiency for various working fluids was a minorant of the critical temperature, and wet fluids were regarded as inappropriate for ORC systems due to hydrogen bond in wet fluids. Through thermodynamically screening 31 pure component working fluids for ORCs, Saleh et al. [19] revealed that lower values of volume flow rate increase thermal efficiency. Victor et al. [20] investigated pure and mixed working fluids for ORCs, and found that the efficiency of a pure ORC working fluid was higher with that of a mixed fluid. Furthermore, Garg et al. [21] applied hydrocarbons blended with CO_2 as the ORC working fluid to suppress the flammability of pure working fluids, so the ORC could operates at a higher temperature level. Wang et al. [22] proposed a thermal efficiency model of the ORC, revealing that the Jakob

* Corresponding authors. Tel.: +86 27 87542618; fax: +86 27 87540724.
E-mail addresses: xmhuang@hust.edu.cn (X.M. Huang), w_liu@hust.edu.cn (W. Liu).

http://dx.doi.org/10.1016/j.energy.2014.06.040
0360-5442/

number played an essential role in the thermal efficiency for various working fluids. To step further, Kuo et al. [23] proposed a new concept named "figure of merit" to discriminate working fluids based on thermal efficiency. In addition Exergy analysis could also bring an insight into the system's thermodynamic perfection degree and the quantitative magnitudes of irreversibility. Many efforts have been focused on the exergy performance of energy converter systems [24–30]. Zhu et al. [26] investigated the exergy destruction and exergy flow map of a bottoming ORC to recover waste heat from the engine exhaust gas. Furthermore the exergy destruction in each components and the exergy efficiency of the ORC system was also studied by Kaska [25], Sun et al. [28] and Borsukiewicz-Gozdur [31], the exergy analysis could provide great guidance to improve the utilization of low grade heat source by using ORCs.

The GA (genetic algorithm) is employed to solve the optimization problem which is based on the theory of the natural selection in the biological genetic progress developed by Charles Darwin. Compared with the traditional optimization techniques, it can deal with complex optimization problem such as nonlinear or discrete problems. The GA considers every parameter as a gene and a solution as a chromosome by encoding them to a specific domain [32]. A number of chromosome-like structures constitute a population. The GA uses three genetic operators to achieve the optimum solution, i.e., selection, crossover and mutation with a randomly generated population. The operations will be terminated while the criterion (fitness function) is fulfilled. The GA method could not only apply to one objective optimization but also multi-objective optimization. The main shortcoming of the GA method is that the computing time will be a little longer if the number of chromosomes is too large or the parameters to be optimized are too more. In order to obtain optimal parameters of the ORC system, performance optimization based on GA (genetic algorithm) has been conducted by many researchers [11,30,32–34]. Larsen et al. [33] studied the optimum parameters of an ORC system for marine engine heat recovery with weighted compromise solution enabling multiple objectives. Wang et al. [11] studied a regenerative ORC to utilize solar energy, using daily average efficiency as the objective function. Wang et al. [34] conducted multi-objective optimization by selecting the exergy efficiency and overall capital cost as the objective functions in studying a traditional ORC for low grade waste heat recovery. Wang et al. [32] applied the ratio of net power output to the total heat transfer area as the objective function to study the ORC performance for the heat recovery of the exhaust gas. Xi et al. [30] chose exergy efficiency as the objective function in optimizing a regenerative ORC. In addition, Papadopoulos et al. [35] adopted computer-aided molecular design and process optimization techniques to select optimal working fluids for ORC. Parameter optimization and performance in subcritical, transcritical and supercritical ORCs have also been investigated [22,36–38].

Many of the aforementioned research works regarding screening appropriate working fluids for ORCs have focused on maximizing the thermal efficiency, and some theoretical models have been proposed to select working fluids based on thermal efficiency. However, exergy efficiency is a more practical criterion to evaluate the utilization of waste heat recovery. In this paper, the internal and external exergy efficiencies are adopted to analyze the impact of the properties of the working fluids in ORC systems. In addition, the overall exergy efficiency has a maximum value according to its definition. The GA method can be used to obtain the maximum overall exergy efficiency and the relative evaporation temperature. Therefore an optimal analysis of ORCs is conducted under different inlet temperatures of heat source with the maximum exergy efficiency as the objective function. Comparisons of the different exergy efficiencies of various working fluids under optimal conditions are also discussed to establish a criterion for selecting the working fluids.

2. Thermodynamic analysis of the ORC

As shown in Fig. 1(a), a typical ORC system consists mainly of a pump, an evaporator, an expander, and a condenser. The working fluid absorbs heat from the heat source, evaporates in the evaporator, and emits heat to the cooling water in the condenser. The vapor from the outlet of the evaporator goes into the expander and drives the shaft rotation to generate electricity. As superheating in the ORC will not increase the exergy efficiency [39–41], in this paper, the working fluid at the expander inlet is saturated for the simulation. Meanwhile, some assumptions are adopted: (1) the system operates under steady state, (2) there is no pressure drop in the connecting pipes and heat exchangers, (3) there is no heat loss in the system, and (4) the isentropic efficiency of the pump is 1.0. The T–s diagram of such a cycle is shown in Fig. 1(b). The thermodynamic analysis of each process can be described as follows.

Work consumption in the pump (process 3 to 4):

$$\dot{W}_p = \dot{m}_f(h_4 - h_3) \tag{1}$$

Heat transfer in the evaporator (process 4 to 1):

$$\dot{Q} = \dot{m}_f(h_1 - h_4) \tag{2}$$

Exergy destruction in the evaporator:

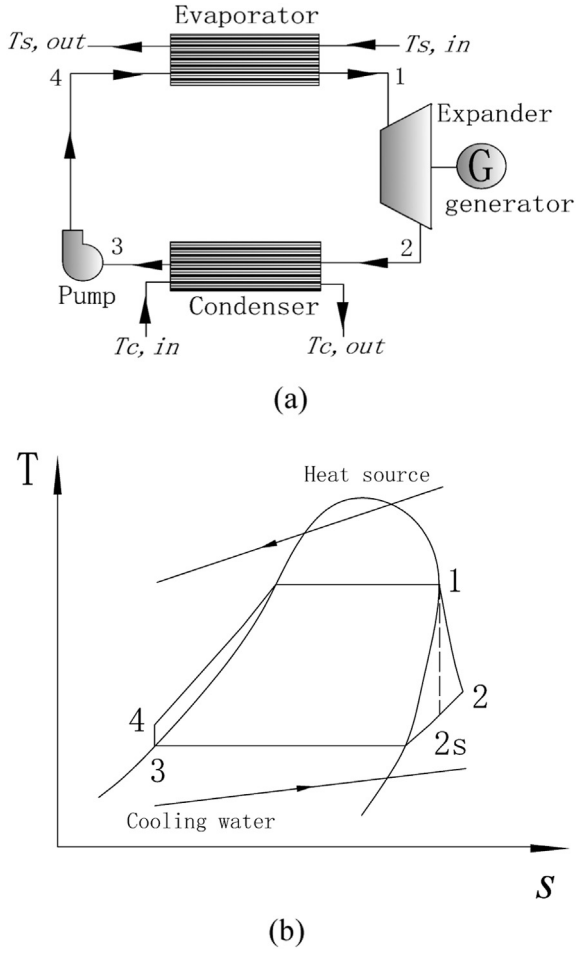

Fig. 1. Schematic diagram of a typical ORC (a) and T–S diagram (b).

$$\dot{I}_{evap} = T_0\left[\dot{m}_f(s_1 - s_4) - \dot{m}_s(s_{s,in} - s_{s,out})\right] \quad (3)$$

Work output in the expander (process 1 to 2):

$$\dot{W}_t = \dot{m}_f(h_1 - h_2) \quad (4)$$

Exergy destruction in the expander:

$$\dot{I}_{exp} = T_0\dot{m}_f(s_2 - s_1) \quad (5)$$

Exergy destruction in the condenser:

$$\dot{I}_{cond} = T_0\left[\dot{m}_f(s_2 - s_3) - \dot{m}_c(s_{c,in} - s_{c,out})\right] \quad (6)$$

Combined with Eqs. (3)–(6), the total exergy destruction of the ORC is described as

$$\dot{I}_{total} = \dot{I}_{evap} + \dot{I}_{exp} + \dot{I}_{cond} \quad (7)$$

The thermal efficiency is defined as

$$\eta_{th} = \frac{\dot{W}_t - \dot{W}_p}{\dot{Q}} \quad (8)$$

The overall exergy efficiency is defined as

$$\eta_{ex} = \frac{\dot{W}_t - \dot{W}_p}{Ex_{s,in}} \quad (9)$$

where the inlet exergy of the heat source is

$$Ex_{s,in} = \dot{m}_s\left[(h_{s,in} - h_{s,0}) - T_0(s_{s,in} - s_{s,0})\right] \quad (10)$$

Here the heat source's exergy at the outlet of the evaporator is treated as exergy loss. Compared with the traditional exergy efficiency, in this paper the total source exergy input for the evaporator is concerned to be the cost of the system. For the same heat source, characteristics of the heat transfer processes are different due to the physical properties of different working fluids, and the outlet condition of the source is also different. Therefore, it would be more insightfully to choose the inlet exergy of the heat source as the total exergy input of the system when the working fluid choosing is concerned.

Furthermore the overall efficiency can be written as the multiplication of two partial efficiencies, i.e.:

$$\eta_{ex} = \eta_{ex,e}\eta_{ex,i} \quad (11)$$

where $\eta_{ex,e}$ and $\eta_{ex,i}$ are respectively external exergy efficiency and the internal efficiency of the ORC. Their definitions are defined as follows:

$$\eta_{ex,e} = \frac{\Delta Ex_{f,evap}}{Ex_{s,in}} \quad (12)$$

$$\eta_{ex,i} = \frac{\dot{W}_{net}}{\Delta Ex_{f,evap}} \quad (13)$$

The external exergy efficiency $\eta_{ex,e}$ denotes the ratio of exergy transferred to the working fluid from the heat source and the inlet exergy of the heat source. When the inlet condition of the heat source is given, it depends primarily on the characteristics of the heat and exergy transfer process in the evaporator and properties of the working fluid. The internal exergy efficiency indicates the exergy efficiency of the fluid cycle, which is determined by the evaporation and condensing temperatures, isentropic efficiencies of the pump and expander, and the thermophysical properties of the working fluid.

To study further the impact of working fluids on the energy conversion of the ORC, the internal and external efficiencies are analyzed separately in the following.

3. Analysis of the internal exergy efficiency

3.1. A simplified model

To illuminate the working fluid's role in the internal exergy efficiency more insightfully, a theoretical model is proposed to evaluate the internal exergy efficiency of the ORC. For simplicity, the power consumed by the pump is neglected; therefore, the internal exergy efficiency of the ORC can be expressed as

$$\eta_{ex,i} = \frac{W_{net}}{\Delta Ex_{f,41}} \quad (14)$$

where $\Delta Ex_{f,41}$ is the exergy augmentation of the working fluid in the evaporator, which can be calculated by

$$\Delta Ex_{f,41} = q_{41} - T_0(s_1 - s_4) \quad (15)$$

The heat transferred to the ORC is

$$q_{41} \approx q_{31} = \overline{C}_p(T_1 - T_3) + \gamma_e \quad (16)$$

The entropy change of the working fluid from state point 4 to 1 can be calculated approximately as

$$s_1 - s_4 \approx \overline{C}_p \ln\frac{T_1}{T_3} + \frac{\gamma_e}{T_1} \quad (17)$$

The network of the ORC is

$$W_{net} = (h_1 - h_{2s})\eta_t = (q_{41} - q_{2s3})\eta_t \quad (18)$$

where η_t is the isentropic efficiency of the expander. The heat rejected to the condenser for isentropic expansion is

$$q_{2s3} = \overline{C}_p(T_{2s} - T_3) + \gamma_c \quad (19)$$

According to the Watson relation [42], the relation between evaporating and condensing latent heat is

$$\gamma_e = \gamma_c\left(\frac{1 - T_e/T_{cr}}{1 - T_c/T_{cr}}\right)^n \quad (20)$$

where $n = 0.38$, T_{cr} is the critical temperature, γ_e and γ_c are the values of latent heat under the saturated temperatures of T_e and T_c, respectively.

Combining Eqs. 14–20, the internal exergy efficiency can be deduced as

$$\eta_{ex,i} = \left(1 - \frac{\frac{B-TEC^{-1}}{1-TEC^{-1}} + (AJa)^{-1} - \frac{TCA/TEC}{1-TEC^{-1}}\ln TEC - TCA/TEC/Ja}{1 + Ja^{-1} - \frac{TCA/TEC}{1-TEC^{-1}}\ln TEC - TCA/TEC/Ja}\right)\eta_t \quad (21)$$

where Ja is the Jakob number, which characterizes the ratio of sensible heat and the latent heat of evaporation, and TEC and TCA are defined as the ratio of evaporating temperature and condensing temperature (T_1/T_3) and the ratio of condensing temperature and ambient temperature (T_3/T_0), respectively. The non-dimensional parameters in Eq. (21) are defined as follows:

$$B = \exp\left(\frac{-\mathrm{TEC}}{A\mathrm{Ja}} + \mathrm{Ja}^{-1} + A^{-1}\mathrm{Ja}^{-1} - \mathrm{TEC}^{-1}\mathrm{Ja}^{-1}\right) \tag{22}$$

$$\mathrm{Ja} = \frac{\overline{C}_p(T_1 - T_3)}{\gamma_e} \tag{23}$$

$$A = \left(\frac{1 - T_1/T_{cr}}{1 - T_3/T_{cr}}\right)^n \tag{24}$$

Meanwhile, the thermal efficiency can also be deduced as

$$\eta_{th} = \left(1 - \frac{\frac{B-\mathrm{TEC}^{-1}}{1-\mathrm{TEC}^{-1}} + (A\mathrm{Ja})^{-1}}{1 + \mathrm{Ja}^{-1}}\right)\eta_t \tag{25}$$

3.2. The validity of the proposed model

To validate the model, the results calculated by Eqs. (21) and (25) are compared with theoretical data from REFPROP [43]. To avoid blade corrosion by the wet fluids in the expander, only dry and isentropic fluids are considered in this paper. The fluid candidates are displayed in Table 1. The comparisons of the thermal and internal exergy efficiencies of the present models and the theoretical data are presented in Fig. 2. Excellent accordance between the proposed model and the theoretical data for different working fluids is observed. Among the working fluids, R141b is an isentropic fluid and R245fa is a dry fluid. The maximum thermal efficiency error in this model is smaller than 2.1% compared with the theoretical data for R245fa, and less than 0.5% for R600a. For the maximum internal exergy efficiency, the error is less than 0.3% for R245fa and 0.32% for R141b in comparison with the theoretical data.

3.3. Parameters influence analysis

According to Eq. (21), the internal exergy efficiency of the ORC is affected mainly by the Jakob number, TEC, and TCA. As the condensing temperature is determined by cooling conditions and the ambient temperature is always treated as constant, no further discussions regarding TCA are presented here. For different working fluids, Fig. 3 illustrates the relation of internal exergy efficiency against the Jakob number and TEC. Each state corresponds to a given evaporation temperature. The evaporation temperature varies from 323 to 403 K, while the condensing temperature T_3 is maintained at a constant 303 K. The ambient temperature T_0 is 293.15 K, which is also treated as constant.

Table 1
Properties of the working fluids studied in this paper.

Working fluid	Fluid type	Critical temperature	Normal boiling temperature	Molecular weight	ODP	GWP
		K	K	kg/kmol		
n-Pentane	Dry	433.75	282.65	72.15	0	~20
R601a	Dry	469.65	300.95	72.15	0	~20
R142b	Isentropic	410.35	263.85	100.49	0.065	2400
Isobutene	Isentropic	418.05	266.25	56.11	–	–
R600a	Isentropic	407.85	261.41	58.12	0	~20
R141b	Isentropic	477.65	305.2	116.95	0.11	630
Butane	Dry	425.15	272.63	58.12	0	~20
R123	Isentropic	456.85	300.95	152.93	0.012	77
R245ca	Dry	447.57	298.28	134.05	0	560
R245fa	Dry	427.21	288.29	134.05	0	820

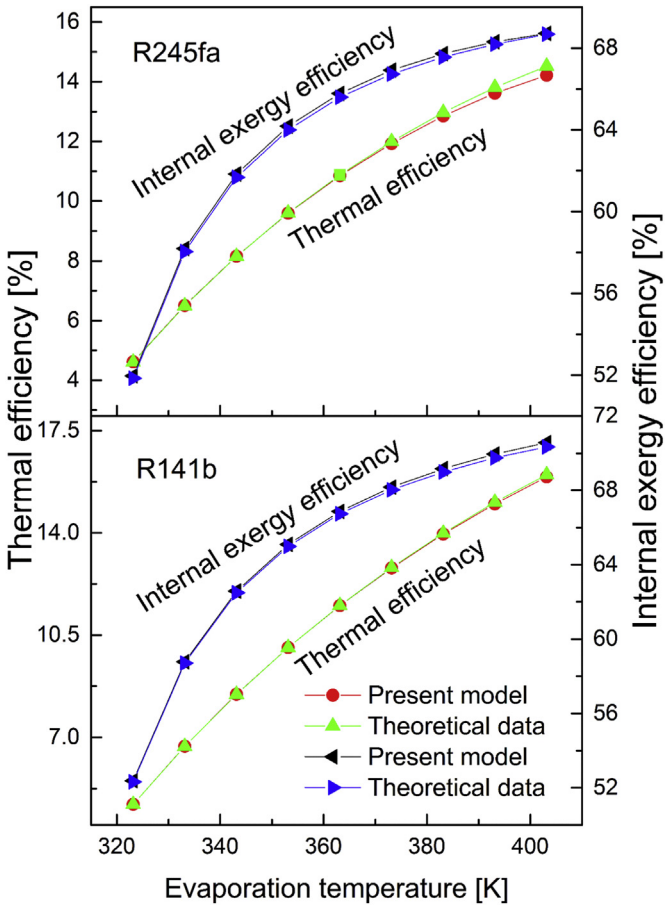

Fig. 2. Comparisons between the results of the present simplified model and the theoretical data ($\eta_t = 0.8$).

Among the three impact parameters of the internal exergy efficiency, the Jakob number is the only one determined by the thermophysical properties of the working fluids. As shown in Fig. 3(a), when the Jakob number is small ($0 < \mathrm{Ja} < 0.9$), the internal exergy efficiency increases dramatically with increasing Jakob number. When the Jakob number gets larger ($\mathrm{Ja} \geq 0.9$), the internal exergy efficiency levels off for higher Jakob numbers. As the Jakob number reflects the ratio of sensible heat and the latent heat of evaporation, higher evaporation temperatures lead to lower latent heat; hence, the Jacob number will be larger. It is of no necessity to increase the evaporation temperature beyond a certain value, because the internal efficiency will increase little for higher temperatures, and because higher evaporation temperatures mean higher pressure in the ORC, which is limited by leakage risk and operational conditions.

According to Fig. 3(a), under a given evaporation temperature, the working fluid with higher critical temperature (e.g., R141b) always has a smaller Jakob number and yet higher internal exergy efficiency. From Fig. 3(b), the internal exergy efficiencies among various working fluids under the same TEC present very small differences. This indicates that the internal exergy efficiencies are determined mainly by operating conditions such as TEC, rather than the thermophysical properties of the working fluids.

4. Analysis of the external exergy efficiency

In practical situations, higher internal efficiency does not ensure larger exergy efficiency, which is often adopted as the criterion of

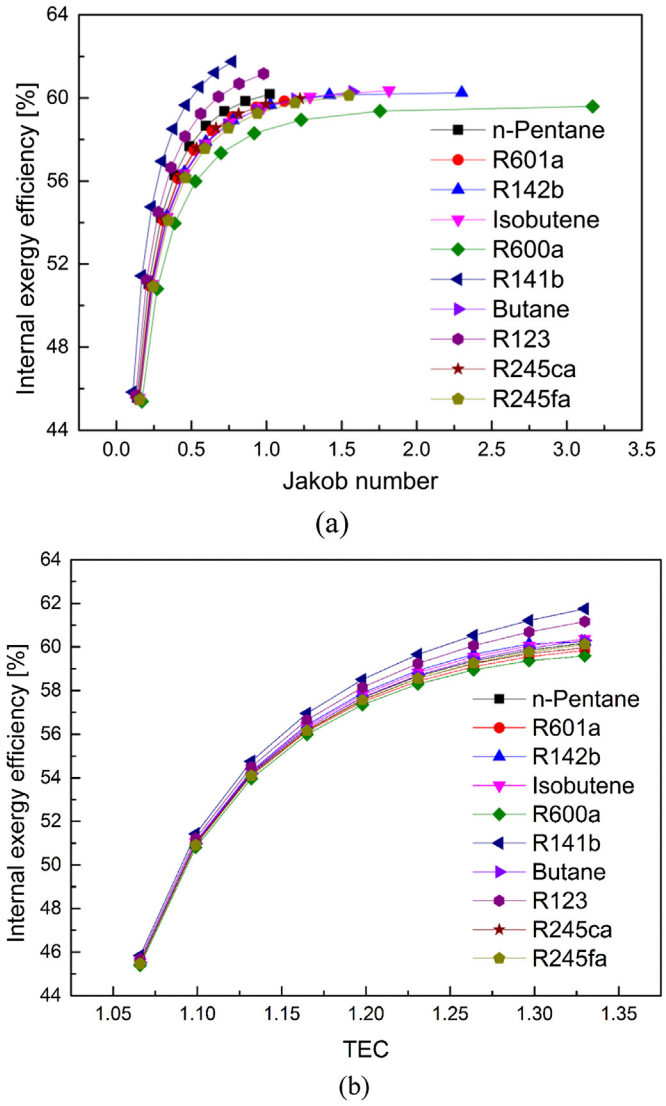

Fig. 3. Internal exergy efficiencies for various working fluids vs Jakob number (a) and TEC (b) ($\eta_t = 0.7$).

the utilization of waste heat recovery. Therefore, the influences on external exergy efficiency are worth analyzing further. However, it is complicated to analyze them theoretically, owing to the characteristics of the various heat sources and the heat transfer performance of the evaporator. In this section, a numerical case for an ORC recovering heat from exhausted fuel gas is presented to analyze the external exergy efficiency. The characteristics of the heat sources are preset by fixing the inlet temperature and mass flow rate, and the performance of the heat transfer process is determined by fixing the pinch point temperature difference of the evaporator. The detailed input parameters are shown in Table 2.

Fig. 4 illustrates the impact of the Jakob numbers on external exergy efficiency. For different working fluids, the external exergy efficiencies present the same tendency; the curves go upwards with increasing Jakob number first, and then decline dramatically beyond a peak point. Therefore, there exists an optimal Jakob number at which the external exergy efficiency achieves the largest value. The optimal Jakob number for different working fluids presents great differences. The optimal external exergy efficiency shifts right and becomes larger for working fluids with lower critical temperature.

Table 2
Input parameters of the ORC.

Parameters	Substitute name	Value
Heat source inlet temperature [K]	$T_{s,in}$	393
Mass flow rate of heat source [kg/s]	$\dot{m}_s$	30
Evaporation temperature [K]	T_{evap}	330–370
Condensing temperature [K]	T_{cond}	303
PPTD in the evaporator [K]	$\Delta T_{pp,e}$	5
Ambient temperature [K]	T_0	293.15
Isentropic efficiency of pump	η_p	1
Isentropic efficiency of expander	η_t	0.5

External exergy efficiency against TEC is displayed in Fig. 5. Because the condensing temperature is treated as a constant in this section, the TEC reflects the evaporation temperature. The characteristics of external exergy efficiency against TEC for all working fluids present parabolic-like curves. The optimal TECs for the maximum external exergy efficiencies of all the working fluids are approximately equal, which are very close to 1.14. Furthermore, the properties of the working fluids exhibit significant effects on the external exergy efficiencies. The maximum difference of the efficiencies at the same TEC is approximately 8%. Working fluids with lower critical temperature (e.g., R600a) always have greater external exergy efficiency at the same evaporation temperature.

As discussed above, the internal exergy efficiency increases with the Jakob number and levels off for high Jakob numbers, whereas the external exergy efficiency achieves its maximum value at the optimal Jakob number and then declines sharply. As the overall exergy efficiency is the product of these two exergy efficiencies, it can be concluded that for the working fluids investigated here, there exists an optimal Jakob number resulting in the maximum overall exergy efficiency. As the condensing temperature is maintained constant here, this optimal state depends only on the evaporation temperature for a given working fluid.

To study further the impact of working fluids on overall exergy efficiency, optimal analyses for the various working fluids are conducted and discussed in the following section.

5. Optimal analysis

5.1. Optimal algorithm

GAs (genetic algorithms) have been used in science and engineering as adaptive algorithms for solving practical problems and

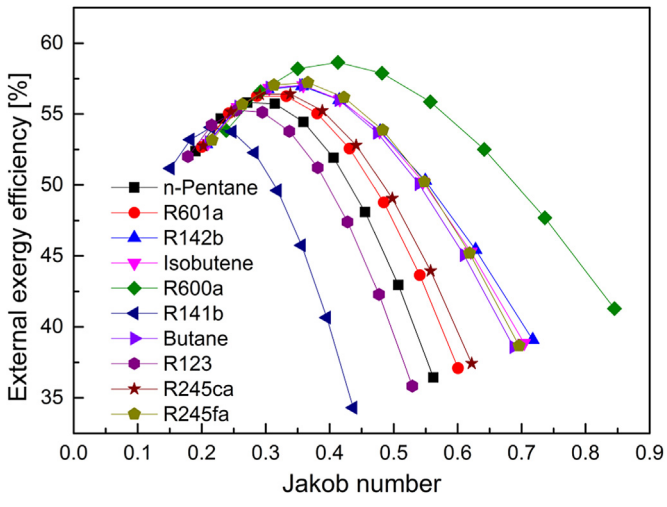

Fig. 4. External exergy efficiency vs Jakob number for different working fluids.

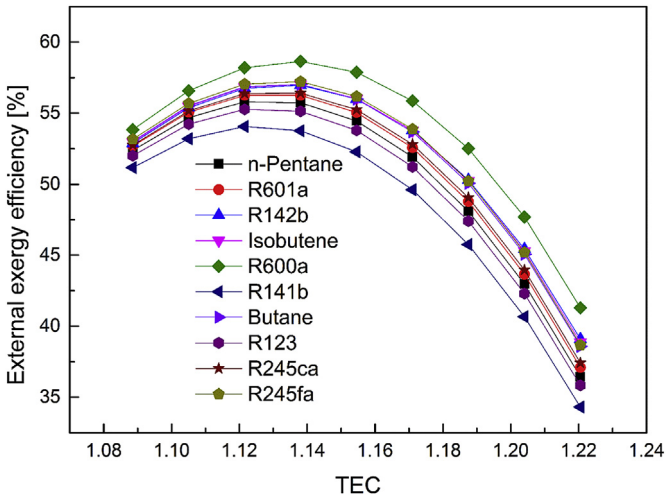

Fig. 5. External exergy efficiency vs TEC for different working fluids.

as computational models of natural evolutionary systems. In this paper, the GA method is employed to obtain optimal parameters of the ORC system for different working fluids by considering the maximum overall exergy efficiency as the objective function. For each case, the heat source inlet parameter and fixed pinch point temperature difference of the evaporator and condenser are given. In the calculation, the temperature of the cooling water and the isentropic efficiencies of the pump and expander are kept constant. The detailed values of these input parameters for the calculation are listed in Table 3.

An ORC with R600a as the working fluid is chosen for this discussion. The characteristics of the exergy efficiencies and exergy destructions with evaporation temperature are displayed in Fig. 6. The overall exergy efficiency characteristics are parabolic-like curves with the increase of evaporation temperature, and an optimal evaporation temperature exists at which maximum overall exergy efficiencies are achieved. For a given working fluid, the optimal evaporation temperature depends on the heat source input temperature.

In Fig. 6(a), the external and internal exergy efficiencies plotted against the evaporation temperature show different patterns. The external exergy efficiencies are larger than the internal exergy efficiencies at different temperatures, except for the temperature point of 370 K. As a consequence, the overall exergy efficiency is dominated mainly by the external exergy efficiency.

Fig. 6(b) shows that the majority of exergy destruction is produced in the evaporator and expander. At lower evaporation temperatures, the exergy destruction in the evaporator accounts for a dominant percentage for the total exergy destruction, while it declines rapidly with increasing evaporation temperature. For higher

Table 3
The input parameters of the ORC in this section.

Parameters	Substitute name	Value
Heat source inlet temperature [K]	$T_{s,in}$	363–423
Mass flow rate of heat source [kg/s]	$\dot{m}_s$	30
Inlet temperature of cooling water [K]	$T_{c,in}$	293.15
Mass flow rate of cooling water[kg/s]	$\dot{m}_c$	70
PPTD in the evaporator [K]	$\Delta T_{pp,e}$	5
PPTD in the condenser [K]	$\Delta T_{pp,c}$	5
Ambient temperature [K]	T_0	293.15
Isentropic efficiency of pump	η_p	1
Isentropic efficiency of expander	η_t	0.5

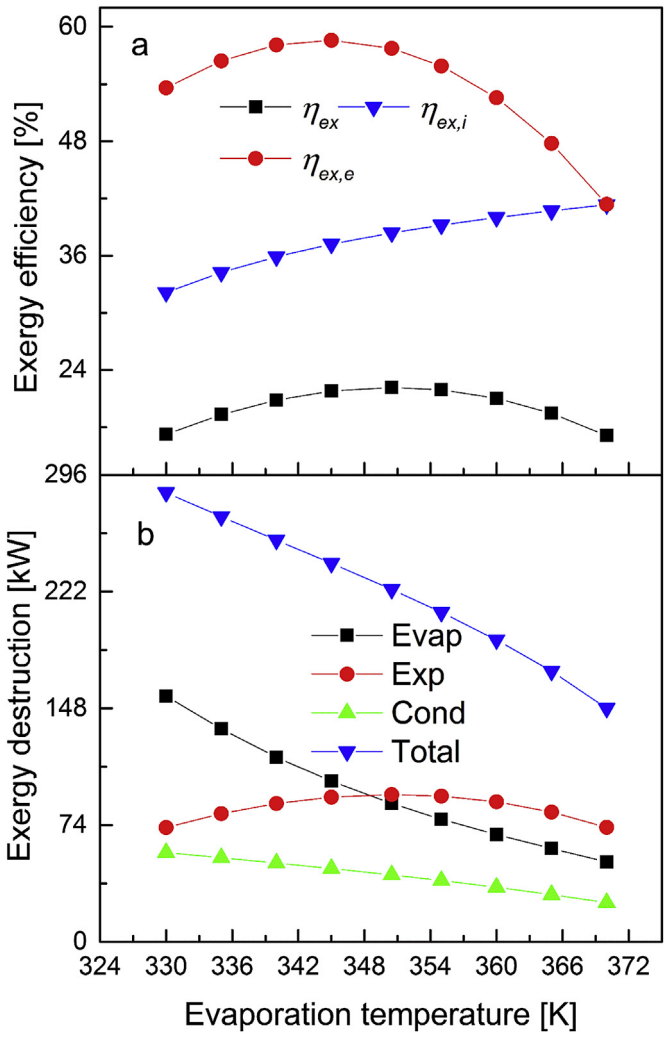

Fig. 6. Exergy efficiency and exergy destruction vs evaporation temperature for R600a ($T_{s,in}$ = 393.15 K; Evap for evaporator; Exp for expander; Cond for condenser).

evaporation temperatures, the expander contributes most to the total exergy destruction. The total exergy destruction decreases sharply with the increase of evaporation temperature due mainly to the decline of the exergy destruction in the evaporator.

Furthermore, the temperatures at which the external and overall exergy efficiencies reach their respective maximum values are very close to each other. This reveals that the determinant impact of the optimal exergy efficiency is the process of heat and exergy transfer between the heat source and working fluid in the evaporator, rather than the working fluid cycle in the ORC. The overall exergy transfer characteristics of the ORC depend greatly on the optimal design of the evaporator. Thus, an optimal evaporation temperature and well-selected working fluid play significant roles in improving the exergy transfer characteristics in the evaporator and therefore, on the performance of the cycle.

5.2. Analysis based on the optimal results

Fig. 7 displays the exergy efficiency, external exergy efficiency, and internal exergy efficiency with heat source inlet temperature for different working fluids under optimal conditions. All the efficiencies rise with increasing inlet temperature of the heat source. For R600a, $\eta_{ex,e}$ increases from 49.8% to 67.5%, as the inlet

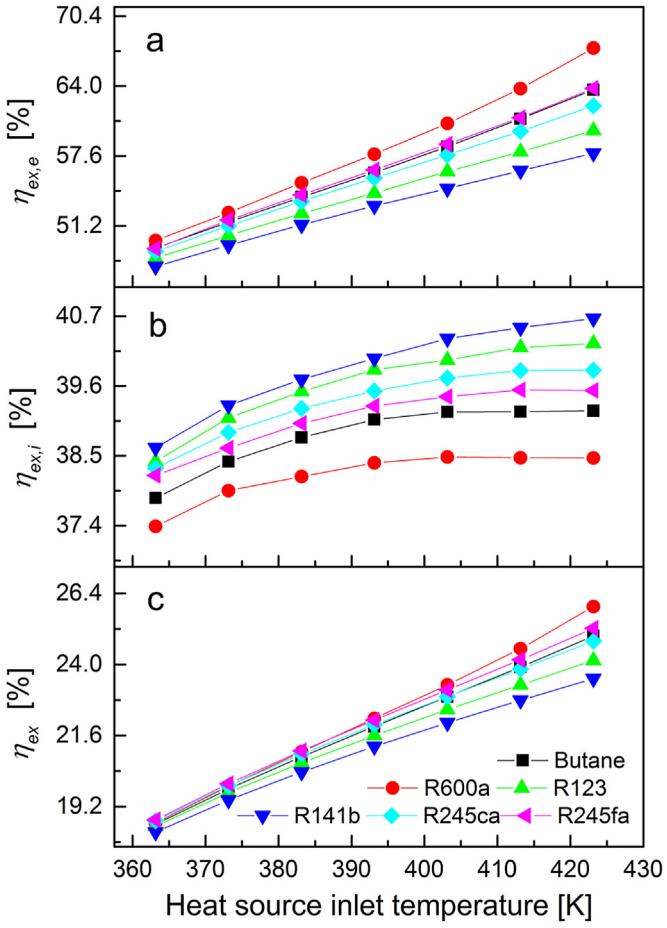

Fig. 7. Exergy efficiency (η_{ex}), external exergy efficiency ($\eta_{ex,e}$), and internal exergy efficiency ($\eta_{ex,i}$) vs heat source inlet temperature for different working fluids under optimal conditions.

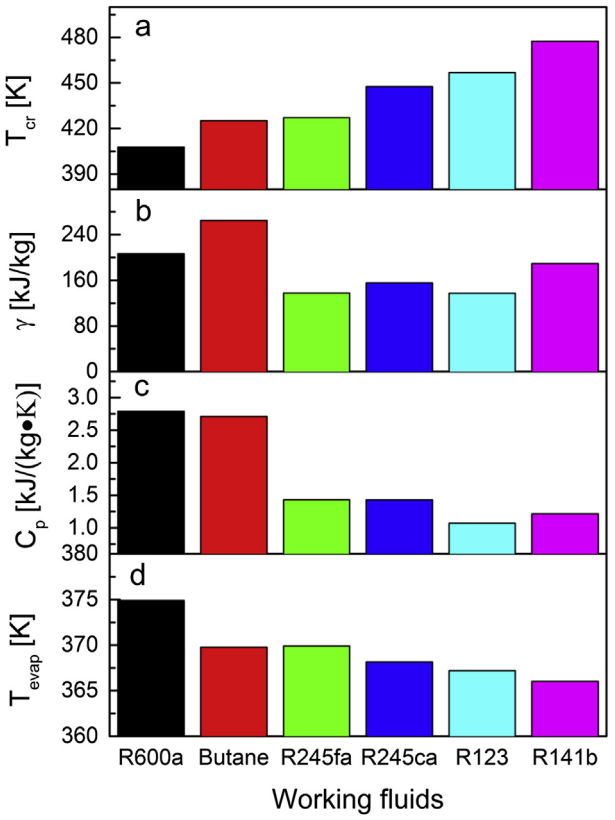

Fig. 8. Comparison of optimal evaporation temperatures and thermophysical properties for different working fluids ($T_{s,in}$ = 423 K).

temperature of the heat source ranges from 363 to 423 K, while $\eta_{ex,i}$ increases relatively slowly from 37.4% to 38.5%. Furthermore, the thermodynamic properties of the working fluids have opposite impacts on the external and internal exergy efficiencies under optimal conditions. At the same inlet temperature, the ORC with R600a as the working fluid has the largest external and overall exergy efficiencies, whereas it has the lowest internal exergy efficiency. However, the trend of the overall exergy efficiency shows considerable agreement with the external exergy efficiency for different working fluids. This analysis provides a further illustration of the determinative impact of external exergy efficiency on the overall exergy efficiency.

As shown in Fig. 7(c), the overall exergy efficiencies of the different working fluids under each temperature point present the same tendency, i.e., R600a shows the highest efficiency and R141b demonstrates the lowest. To elucidate this phenomenon further, the thermophysical properties of these working fluids and the optimal evaporation temperature are listed in Fig. 8. It can be observed that the latent and specific heat are not the dominant factors in exergy efficiency. For each working fluid, the critical and the optimal evaporating temperature present opposite trends. The working fluid with the highest critical temperature shows the lowest evaporating temperature, as shown in Fig. 8(a) and (d). For a fixed heat source and cooling conditions, the working fluid with a lower critical temperature will present a larger evaporation temperature and therefore, higher exergy efficiency.

6. Conclusions

This paper studies the impact of working fluids on the performance of ORC systems and the selection of working fluids for ORCs by comparing and analyzing the internal and external exergy efficiencies. The calculation results show that the thermophysical properties of the working fluid have little impact on internal exergy efficiency, but they do play an important role in determining external exergy efficiency. With the increase of evaporation temperature, the internal exergy efficiency of the ORC will increase for all working fluids, whereas the characteristics of the external exergy efficiency exhibit parabolic-like curves. Evaporation temperature of the ORC is a principal factor in determining the internal exergy efficiency, rather than the thermophysical properties of the working fluids. However, both the evaporation temperature and the thermophysical properties have significant effects on external exergy efficiency. The optimal analysis conducted for the ORC shows that the working fluid with lower critical temperature has a higher optimal evaporation temperature, which leads to larger overall exergy efficiency.

Acknowledgments

This work is supported by the National Natural Science Foundation of China (No. 51036003) and the National Key Basic Research Development Program of China (No. 2013CB228302).

Nomenclature

h	enthalpy [kJ/kg]
$\dot{m}$	mass flow rate [kg/s]

P	pressure [kPa]
$\dot{Q}$	heat rate [kW]
s	entropy [kJ/(kg K)]
T	temperature [K]
$\dot{W}$	work [kW]
c_p	specific heat [kJ/(kg K)]
$\dot{I}$	exergy destruction [kW]
$\dot{E}x$	exergy rate [kW]

Greek symbols

η_{th}	thermal efficiency
η_{ex}	overall exergy efficiency
$\eta_{ex,e}$	external exergy efficiency
$\eta_{ex,i}$	internal exergy efficiency
γ_e	evaporation latent heat [kJ/kg]
γ_c	thermal efficiency
η_{ex}	overall exergy efficiency
$\eta_{ex,e}$	external exergy efficiency
$\eta_{ex,i}$	internal exergy efficiency
γ_e	evaporation latent heat [kJ/kg]
γ_c	condensing latent heat [kJ/kg]

Subscripts

f	working fluid
0	ambient state
1–5	states in the cycle
s	heat source
c	cold source
cr	critical
p	pump
evap	evaporator
in	inlet
out	outlet
exp	expander
cond	condenser

Acronyms

PPTD	pinch point temperature difference
GWP	global warming potential
ODP	ozone depletion potential
ORC	organic Rankine cycle
TEC	ratio of evaporating temperature and condensing temperature
TCA	ratio of condensing temperature and ambient temperature
GA	genetic algorithm

References

[1] Wang R, Yu X, Ge T, Li T. The present and future of residential refrigeration, power generation and energy storage. Appl Therm Eng 2013;53(2):256–70.
[2] Li G. Review of thermal energy storage technologies and experimental investigation of adsorption thermal energy storage for residential application [Master thesis]. College Park: University of Maryland; 2013.
[3] Li G, Hwang Y, Radermacher R. Review of cold storage materials for air conditioning application. Int J Refrig 2012;35(8):2053–77.
[4] Li G, Hwang Y, Radermacher R, Chun H-H. Review of cold storage materials for subzero applications. Energy 2013;51:1–17.
[5] Li G, Qian S, Lee H, Hwang Y, Radermacher R. Experimental investigation of energy and exergy performance of short term adsorption heat storage for residential application. Energy 2014;65(0):675–91.
[6] Singh R, Miller SA, Rowlands AS, Jacobs PA. Dynamic characteristics of a direct-heated supercritical carbon-dioxide Brayton cycle in a solar thermal power plant. Energy 2013;50:194–204.
[7] Ho T, Mao SS, Greif R. Comparison of the Organic Flash Cycle (OFC) to other advanced vapor cycles for intermediate and high temperature waste heat reclamation and solar thermal energy. Energy 2012;42(1):213–23.
[8] Steffen M, Löffler M, Schaber K. Efficiency of a new Triangle Cycle with flash evaporation in a piston engine. Energy 2013;57:295–307.
[9] Franco A, Vaccaro M. On the use of heat pipe principle for the exploitation of medium–low temperature geothermal resources. Appl Therm Eng 2013;59(1):189–99.
[10] Tchanche BF, Lambrinos G, Frangoudakis A, Papadakis G. Low-grade heat conversion into power using organic Rankine cycles – a review of various applications. Renew Sustain Energy Rev 2011;15(8):3963–79.
[11] Wang M, Wang J, Zhao Y, Zhao P, Dai Y. Thermodynamic analysis and optimization of a solar-driven regenerative organic Rankine cycle (ORC) based on flat-plate solar collectors. Appl Therm Eng 2013;50(1):816–25.
[12] Sprouse III C, Depcik C. Review of organic Rankine cycles for internal combustion engine exhaust waste heat recovery. Appl Therm Eng 2013;51(1):711–22.
[13] Macián V, Serrano J, Dolz V, Sánchez J. Methodology to design a bottoming Rankine cycle, as a waste energy recovering system in vehicles. Study in a HDD engine. Appl Energy 2013;104:758–71.
[14] Vetter C, Wiemer H-J, Kuhn D. Comparison of sub-and supercritical Organic Rankine Cycles for power generation from low-temperature/low-enthalpy geothermal wells, considering specific net power output and efficiency. Appl Therm Eng 2013;51(1):871–9.
[15] Vatani A, Khazaeli A, Roshandel R, Panjeshahi MH. Thermodynamic analysis of application of organic Rankine cycle for heat recovery from an integrated DIR-MCFC with pre-reformer. Energy Convers Manag 2013;67:197–207.
[16] Hung T, Shai T, Wang S. A review of organic Rankine cycles (ORCs) for the recovery of low-grade waste heat. Energy 1997;22(7):661–7.
[17] Hung T, Wang S, Kuo C, Pei B, Tsai K. A study of organic working fluids on system efficiency of an ORC using low-grade energy sources. Energy 2010;35(3):1403–11.
[18] Liu B-T, Chien K-H, Wang C-C. Effect of working fluids on organic Rankine cycle for waste heat recovery. Energy 2004;29(8):1207–17.
[19] Saleh B, Koglbauer G, Wendland M, Fischer J. Working fluids for low-temperature organic Rankine cycles. Energy 2007;32(7):1210–21.
[20] Victor RA, Kim J-K, Smith R. Composition optimisation of working fluids for Organic Rankine cycles and Kalina cycles. Energy 2013;55:114–26.
[21] Garg P, Kumar P, Srinivasan K, Dutta P. Evaluation of carbon dioxide blends with isopentane and propane as working fluids for organic Rankine cycles. Appl Therm Eng 2013;52(2):439–48.
[22] Wang D, Ling X, Peng H, Liu L, Tao L. Efficiency and optimal performance evaluation of organic Rankine cycle for low grade waste heat power generation. Energy 2013;50:343–52.
[23] Kuo C-R, Hsu S-W, Chang K-H, Wang C-C. Analysis of a 50kW organic Rankine cycle system. Energy 2011;36(10):5877–85.
[24] Janghorban Esfahani I, Yoo C. Exergy analysis and parametric optimization of three power and fresh water cogeneration systems using refrigeration chillers. Energy 2013;59:340–55.
[25] Kaşka Ö. Energy and exergy analysis of an organic Rankine for power generation from waste heat recovery in steel industry. Energy Convers Manag 2014;77:108–17.
[26] Zhu S, Deng K, Qu S. Energy and exergy analyses of a bottoming Rankine cycle for engine exhaust heat recovery. Energy 2013;58:448–57.
[27] El-Emam RS, Dincer I. Exergy and exergoeconomic analyses and optimization of geothermal organic Rankine cycle. Appl Therm Eng 2013;59(1):435–44.
[28] Sun F, Ikegami Y, Jia B, Arima H. Optimization design and exergy analysis of organic rankine cycle in ocean thermal energy conversion. Appl Ocean Res 2012;35:38–46.
[29] Garcia-Hernando N, de Vega M, Soria-Verdugo A, Sanchez-Delgado S. Energy and exergy analysis of an absorption power cycle. Appl Therm Eng 2013;55(1):69–77.
[30] Xi H, Li M-J, Xu C, He Y-L. Parametric optimization of regenerative organic Rankine cycle (ORC) for low grade waste heat recovery using genetic algorithm. Energy 2013;58:473–82.
[31] Borsukiewicz-Gozdur A. Exergy analysis for maximizing power of organic Rankine cycle power plant driven by open type energy source. Energy 2013;62:73–81.
[32] Wang J, Yan Z, Wang M, Ma S, Dai Y. Thermodynamic analysis and optimization of an (organic Rankine cycle) ORC using low grade heat source. Energy 2013;49:356–65.
[33] Larsen U, Pierobon L, Haglind F, Gabrielii C. Design and optimisation of organic Rankine cycles for waste heat recovery in marine applications using the principles of natural selection. Energy 2013;55:803–12.
[34] Wang J, Yan Z, Wang M, Li M, Dai Y. Multi-objective optimization of an organic Rankine cycle (ORC) for low grade waste heat recovery using evolutionary algorithm. Energy Convers Manag 2013;71:146–58.
[35] Papadopoulos AI, Stijepovic M, Linke P. On the systematic design and selection of optimal working fluids for Organic Rankine cycles. Appl Therm Eng 2010;30(6):760–9.
[36] He C, Liu C, Gao H, Xie H, Li Y, Wu S, et al. The optimal evaporation temperature and working fluids for subcritical organic Rankine cycle. Energy 2012;38(1):136–43.
[37] Schuster A, Karellas S, Aumann R. Efficiency optimization potential in supercritical Organic Rankine cycles. Energy 2010;35(2):1033–9.
[38] Shengjun Z, Huaixin W, Tao G. Performance comparison and parametric optimization of subcritical Organic Rankine cycle (ORC) and transcritical power cycle system for low-temperature geothermal power generation. Appl Energy 2011;88(8):2740–54.

[39] Roy J, Mishra M, Misra A. Parametric optimization and performance analysis of a waste heat recovery system using Organic Rankine cycle. Energy 2010;35(12):5049–62.
[40] Mago PJ, Chamra LM, Srinivasan K, Somayaji C. An examination of regenerative organic Rankine cycles using dry fluids. Appl Therm Eng 2008;28(8):998–1007.
[41] Roy J, Mishra M, Misra A. Performance analysis of an Organic Rankine cycle with superheating under different heat source temperature conditions. Appl Energy 2011;88(9):2995–3004.
[42] Poling BE, Prausnitz JM, O'Connell JP. The properties of gases and liquids. 5th ed. New York: McGraw-Hill; 2001.
[43] Lemmon EW, Huber ML, McLinden MO. NIST standard reference database 23: reference fluid thermodynamic and transport properties-REFPROP, version8.0. Gaithersburg: National Institute of Standards and Technology; 2007. Standard Reference Data Program.